JOURNAL OF THE BULGARIAN GEOGRAPHICAL SOCIETY

Journal of the Bulgarian Geographical Society 50: 95–112 (2024)
DOI: 10.3897/jbgs.e124098

Research Article

Exploring the relationship between remote sensing-based vegetation indices and land surface temperature through quantitative analysis

Ibrahim Olatunji Raufu[1]

1 *Department of Surveying and Geoinformatics, Federal University of Technology Akure, Akure, Nigeria*
Corresponding author: Ibrahim Olatunji Raufu (raufuibrahimolatunji@gmail.com)

Abstract

In an era of rapid urbanization, understanding the complex relationship between vegetation dynamics and land surface temperature (LST) is crucial for addressing the challenges posed by urban heat island (UHI) and promoting sustainable urban development. Our study aimed to explore these dynamics in a rapidly urbanizing environment by analyzing the relationships between remote sensing-based vegetation indices and LST through quantitative analysis. A cloud-free Landsat 8 OLI/TIRS level 2 satellite imagery of Ibadan region city for 2022 was obtained from the United State Geological Survey (USGS) and LST was estimated using the radiative transfer approach. Utilizing different combinations of spectral bands, seven vegetation indices including Normalized Difference Vegetation Index (NDVI), Soil Adjusted Vegetation Index (SAVI), Atmospherically Resistant Vegetation Index (ARVI), Green Normalized Difference Vegetation Index (GNDVI), Ratio Vegetation Index (RVI), Optimized Soil Adjusted Vegetation Index (OSAVI), and Green Chlorophyll Index (GCI) were analyzed. Combined with the spatial distribution of LST in Ibadan, regression analysis were performed to explore the relationship between vegetation indices and LST. Results indicate that among the seven vegetation indices, ARVI has the strongest correlation with LST in the study area (R^2 = 0.65). Additionally, urban cores experience lower vegetation density and higher LST values, which can be attributed to land use intensity, anthropogenic heat release, and impervious surface cover while the peripheral areas exhibit higher vegetation indices and lower LST values. The findings of this study contribute to a deeper understanding of urban environmental dynamics and provide valuable insights for sustainable urban planning, ecosystem management, and climate adaptation strategies in rapidly urbanizing areas.

Key words: ARVI, GCI, GNDVI, NDVI, OSAVI, RVI, SAVI, urban heat island

OPEN ACCESS

Academic editor: Daniela Avetisyan
Received: 27 March 2024
Accepted: 14 May 2024
Published: 28 May 2024

Citation: Raufu IO (2024) Exploring the relationship between remote sensing-based vegetation indices and land surface temperature through quantitative analysis. Journal of the Bulgarian Geographical Society 50: 95–112. https://doi.org/10.3897/jbgs.e124098

Copyright: © Ibrahim Olatunji Raufu This is an open access article distributed under terms of the Creative Commons Attribution License (Attribution 4.0 International – CC BY 4.0).

1. Introduction

The rapid pace of urbanization, projected by the United Nations to result in over 68% of the global population residing in urban areas by 2050 (United Nations 2018), necessitates significant alterations in land use and land cover to accommodate the expanding urban population's infrastructure needs. This urban expansion exerts an impact on the Earth's surface energy balance, subse-

quently influencing land surface temperature (LST) and leading to shifts in the micro-climate of the region (Wang et al. 2018; Gogoi et al. 2019; Guechi et al. 2021). Changes in land use and land cover, particularly noticeable in urban areas where temperatures exceed those of surrounding vegetated and water-covered regions, have been linked to global temperature rises (Dontree 2010; Fashae et al. 2020; Tan et al. 2020). This phenomenon is attributed to significant reductions in green spaces and the greenhouse effect resulting from fuel combustion in transportation, commerce, manufacturing, and households (Dontree 2010; Kumar et al. 2012; Fashae et al. 2020). Thus, rapid urbanization is increasingly recognized as a significant global challenge due to its diverse socioeconomic and environmental consequences, including strains on infrastructure, ecological degradation, and the urban heat island effect (MacLachlan et al. 2017).

Urban heat island (UHI) is indeed a crucial aspect of urban climate change, with profound implications for human settlements within cities (Wei et al. 2008; Kumar and Shekhar 2015). This phenomenon occur where urban areas experience significantly higher temperatures compared to their surrounding rural areas (Brattebo and Booth 2003; Guechi et al. 2021). This temperature differential is primarily caused by human activities and modifications to the landscape, such as the proliferation of buildings, roads, and other impervious surfaces, which absorb and retain heat during the day and release it at night (Zaeemdar and Baycan 2017; Fashae et al. 2020). Additionally, the reduced vegetation cover in urban areas diminishes the cooling effect of evapotranspiration, further intensifying the heat island effect (Das et al. 2020; Guechi et al. 2021). The UHI effect, characterized by elevated temperatures in cities, poses health risks, increases energy demand, diminishes outdoor comfort, intensifies climate change, and disrupts ecosystems (Grimmond 2007; Plocoste et al. 2014; Guechi et al. 2021). LST is a critical parameter for understanding surface energy balance, urban heat island effects, and climate change impacts (Liu and Zhang 2011).

In contrast to conventional observation methods utilized at meteorological stations, remote sensing offers a powerful tool for monitoring LST across extensive areas with consistent spatial measurements. Remote sensing enables comprehensive assessment of various Earth surface parameters over large spatial extents and temporal scales, facilitating insights into ecosystem dynamics, land cover changes, and climate variability (Bhagyanagar et al. 2012; Firozjaei et al. 2019; Wang 2023). The relationship between remote sensing-based vegetation indices and LST has garnered significant attention in environmental research due to its pivotal role in elucidating the interactions between vegetation dynamics and surface temperature. Understanding the interactions between vegetation dynamics and surface temperature is essential for ecosystem management, agricultural planning, urban development, and climate modeling efforts.

Many research studies have utilized various vegetation parameters, including the Normalized Difference Vegetation Index (NDVI), Enhanced Vegetation Index (EVI), Green Normalized Difference Vegetation Index (GNDVI), Soil-Adjusted Vegetation Index (SAVI), Modified Soil-Adjusted Vegetation Index (MSAVI), Normalized Difference Built-up Index (NDBI), and Ratio Vegetation Index (RVI), to investigate the correlation between LST and vegetation (Yue et al. 2007; Wei et al. 2008; Kumar and Shekhar 2015; Macarof et al. 2018; Guechi

et al. 2021; Aliyu et al. 2022; Ullah et al. 2023; Debele and Beketie 2024). Debele and Beketie (2024) explore the relationships between LST and its driving environmental factors in the Upper Awash Basin (UAB) of Ethiopia by utilizing Landsat 8 OLI/TIRS imagery and ASTER GDEM to generate LST and biophysical factors. The result obtained shows that increased LST was notably influenced by NDBI, while EVI showed negative correlation with LST. In another study by Guechi et al. (2020), the relationship between vegetation parameters and LST was examined using time-series of Landsat images TM, ETM+ and OLI/TIRS data in Algeria. The study reported that a strong negative correlation exists between NDVI, SAVI and LST while a strong positive correlation was found between NDBI and LST. Similarly, negative correlation between NDVI and LST was reported by other studies (Yue et al. 2007; Wei et al. 2008; Kumar and Shekhar 2015; Ullah et al. 2023).

Quantitative analysis of the relationship between vegetation indices and LST offers valuable insights into the underlying processes driving ecosystem functioning and surface temperature dynamics. By examining the spatial and temporal patterns of vegetation indices and LST, researchers can identify spatially explicit vegetation-temperature relationships, assess ecosystem health and resilience, and monitor land surface changes over time. The NDVI, widely utilized in UHI studies, serves as a key indicator of vegetation abundance by leveraging remote sensing to assess the link between vegetation and LST. However, the nonlinear nature of NDVI suggests limitations in its suitability for quantitative analyses of vegetation in exploring the vegetation-LST relationship (Wei et al. 2008; Schwarz et al. 2012; Kumar and Shekhar 2015). Consequently, there is a need for further calibration of the relationship between LST and NDVI. Additionally, there is an emphasis on the importance of identifying a more suitable and robust indicator of vegetation abundance to replace NDVI in studies investigating the relationship between vegetation and LST (Kumar and Shekhar 2015).

The rapid and extensive urban expansion in Ibadan has significantly disrupted the landscape, leading to profound spatial and environmental changes. This expansion is evidenced by the increased built-up areas, population growth, and intensified commercial and transportation activities in the region. In this study, our objective is to investigate the relationship between remote sensing-based vegetation indices and land surface temperature through quantitative analysis within the context of Ibadan city, located in Oyo state, South-Western Nigeria. By integrating satellite imagery, geospatial analysis techniques, and statistical analysis, we aim to elucidate the intricate interactions between vegetation dynamics and surface temperature in a rapidly urbanizing environment.

2. Materials and Methods

2.1. Study area

The study area is Ibadan city, Oyo state in South-Western part of Nigeria. It is situated between latitude 7°02'49"N to 7°43'21"N and longitude 3°31'58"E to 4°08'20"E with an elevation ranges from 180 m to 210 m above the mean sea level. The city has total area of 6,800 sq.km and a population of 3.8 million people as estimated in 2023 by Population Stat (2024). The climate in the study area is characterized by a tropical wet and dry climate, featuring a prolonged

wet season and relatively stable temperatures throughout the year. The city maintains an average annual temperature of 26.46°C. The wet season lasts from March to October, with a brief dry period occurring in August. The natural vegetation cover, especially in the metropolitan area of Ibadan, has largely been replaced by impermeable surfaces, primarily due to rapid population growth and urbanization.

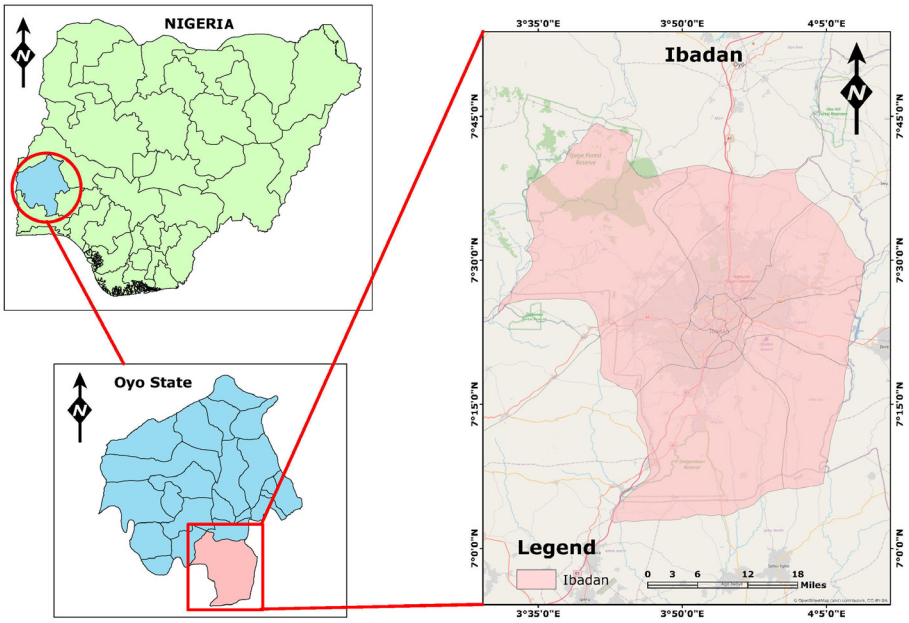

Figure 1. Map showing location of the study area.

2.2. Satellite imagery

Landsat 8 is a pivotal Earth observation satellite jointly operated by NASA and the United States Geological Survey (USGS), contributing to the continuous monitoring and understanding of changes in the Earth's surface since its launch in 2013. Equipped with the Operational Land Imager (OLI) and Thermal Infrared Sensor (TIRS), Landsat 8 captures imagery with remarkable detail and accuracy, facilitating the monitoring of various environmental parameters. With eleven spectral bands covering visible light to thermal infrared and a spatial resolution ranging from 15 to 100 meters (Table 1), Landsat 8 enables detailed assessments of land cover, vegetation health, urban development, and other factors affecting the Earth's surface.

In this study, a cloud-free Landsat 8 OLI/TIRS level 2 satellite imagery that has been radiometrically calibrated and atmospherically corrected was downloaded from the USGS website for December 27, 2022. The choice of this date aligns with the typical dry season period for the study area, where historical weather patterns indicate reduced cloud cover and stable atmospheric conditions. This selection enhances the likelihood of obtaining clear, high-quality imagery with minimal atmospheric interference, ensuring the reliability and accuracy of the data for analysis. The thermal infrared band (band 10) was provided as the atmospheric brightness temperature in Kelvin (K) and all the multispectral bands were provided as surface reflectance.

Table 1. Landsat 8 spectral bands properties (Castaldi 2021).

Band number	Band names	Central wavelength (nm)	Spatial resolution	Possible applications
1	Coastal aerosol	443	30	Water quality assessment
2	Blue	483	30	Vegetation
3	Green	560	30	Vegetation
4	Red	660	30	Vegetation
5	Near-infrared (NIR)	865	30	Vegetation
6	Shortwave infrared (SWIR) 1	1650	30	Soil moisture estimation
7	Shortwave infrared (SWIR) 2	2220	30	Vegetation
8	Panchromatic	590	15	Urban planning
9	Cirrus	1375	30	Atmosphere
10	Thermal infrared (TIRS) 1	10795	100	Thermal mapping
11	Thermal infrared (TIRS) 2	11605	100	Thermal mapping

2.3. Estimation of land surface temperature

The estimation of LST in this study was conducted in three stages. Firstly, the proportion of vegetation (Pv) was estimated using the Normalized Difference Vegetation Index (NDVI) derived from satellite imagery. The formula used is as follows:

$$Pv = \left(\frac{(NDVI - NDVI_{min})}{(NDVI_{max} - NDVI_{min})}\right)^2 \quad (1)$$

where Pv denotes the amount of vegetation, $NDVI_{min}$ denotes the minimum values of the NDVI, and $NDVI_{max}$ denotes the maximum value of the NDVI.

Secondly, the land surface emissivity (ε) was estimated based on the proportion of vegetation (Pv) using the formula proposed by Sobrino et al. (2004):

$$\varepsilon = 0.004 * Pv + 0.986 \quad (2)$$

Emissivity is a material's relative capacity to radiate heat, and it influences the thermal radiation emitted from the land surface.

Thirdly, The Landsat-8 TIRS (band 10) data provided as top-of-atmosphere brightness temperature (Tb) in Kelvin (K) by the USGS, was utilized to calculate LST. The following formular was employed:

$$LST = \left(\frac{T_b}{1 + \left(\lambda \times \frac{T_b}{\rho}\right)\ln(\varepsilon)}\right) \quad (3)$$

Where *Tb* is the top-of-atmosphere brightness temperature, λ is the wavelength of emitted radiance, $\rho = h \times (c/s) = 1.4388 \times 10^{-2}$ m K = 14388 μm K, *h* is the plank's constant = 6.626×10^{-34} Js, *s* is the Boltzmann constant = 1.38×10^{-23} J/K, *c* = velocity of light = 2.998×10^8 m/s.

To convert the radiant temperature to degrees Celsius, a value of 273.15 was subtracted from the calculated temperature

2.4. Vegetation indices

In this study, seven widely-used vegetation indices (Table 2) are analyzed to explore their relationship with LST. Vegetation indices are mathematical formulations derived from spectral bands captured by remote sensing instruments, such as Landsat 8 and Sentinel-2 satellites. These indices provide valuable insights into vegetation properties, health, and dynamics based on the interaction between vegetation and incident light.

Table 2. List of vegetation indices under study.

No.	Indices	Formula	Reference
1	Normalized Difference Vegetation Index (NDVI)	(NIR − Red) / (NIR + Red)	(Rouse et al. 1974)
2	Soil Adjusted Vegetation Index (SAVI)	[(NIR − Red) / (NIR + Red + L)] * (1 + L)	(Huete 1988)
3	Atmospherically Resistant Vegetation Index (ARVI)	(NIR − (2 * Red) + Blue) / (NIR + (2 * Red) + Blue)	(Tanré et al. 1992)
4	Green Normalized Difference Vegetation Index (GNDVI)	(NIR − Green) / (NIR + Green)	(Barati et al. 2011)
5	Ratio Vegetation Index (RVI)	NIR / Red	(Pearson and Miller 1972)
6	Optimized Soil Adjusted Vegetation Index (OSAVI)	1.16 * (NIR − Red) / (NIR + Red + 0.16)	(Rondeaux et al. 1996)
7	Green Chlorophyll Index (GCI)	((NIR / Green)) − 1	(Gitelson et al. 2003)

2.4.1. Normalized difference vegetation index (NDVI)

The NDVI is a widely used vegetation index derived from remotely sensed data, typically captured by satellites. It quantifies the density and strength of green vegetation cover by comparing the reflectance of two spectral bands: the near-infrared (NIR) and the red (Red) bands. NDVI values range from −1 (for snow and ice) to +1 (for complete vegetation cover), providing a quantitative measure of vegetation density and health. NDVI tends to have a more linear relationship with vegetation properties such as biomass or leaf area index (LAI), with higher values indicating denser and healthier vegetation (Kumar and Shekhar 2015). The NDVI is calculated as:

$$NDVI = (NIR - Red) / (NIR + Red) \quad (4)$$

Where NIR represents the reflectance in the near-infrared band and Red represents the reflectance in the red band.

NDVI takes advantage of the differential reflectance properties of vegetation in the near-infrared and red spectral bands. Healthy vegetation reflects a large amount of near-infrared light due to chlorophyll absorption, while absorbing more red light for photosynthesis. Bare soil or non-vegetated areas generally reflect similar amounts of near-infrared and red light (Gutman et al. 2021).

2.4.2. Soil adjusted vegetation index (SAVI)

The SAVI is a modified version of the NDVI designed to reduce the influence of soil brightness variations on vegetation indices. By incorporating a soil adjustment factor, SAVI minimizes the impact of soil background effects, making it particularly useful in areas with diverse soil types or varying soil moisture conditions. The formular for estimating SAVI is as follows:

$$SAVI = [(NIR - Red) / (NIR + Red + L)] * (1 + L) \quad (5)$$

L is a constant factor ranging from 0 to 1, which is used to adjust the soil brightness. Typically, L = 0.5 is used as a default value, as suggested by Huete (1988), to account for first-order soil background variations.

2.4.3. Atmospherically resistant vegetation index (ARVI)

The ARVI is an adapted version of the NDVI that seeks to mitigate the influence of atmospheric conditions on vegetation indices. ARVI is particularly valuable in regions where atmospheric effects, such as aerosols and haze, can distort satellite-derived vegetation assessments. The formula for ARVI is expressed as:

$$ARVI = (NIR - (2 * Red) + Blue) / (NIR + (2 * Red) + Blue) \quad (6)$$

By incorporating the blue band, ARVI accounts for atmospheric influences, such as Rayleigh scattering, which can affect the accuracy of vegetation indices. This adjustment enhances the sensitivity of ARVI to vegetation changes while reducing the impact of atmospheric variability. Its application contributes to improved monitoring of land surface dynamics, environmental changes, and ecosystem health

2.4.4. Green normalized difference vegetation index (GNDVI)

The GNDVI is a vegetation index similar to the NDVI but calculated using green and near-infrared bands instead of red and near-infrared bands. GNDVI is particularly useful in areas where vegetation reflects more strongly in the green band compared to the red band, such as dense forests. According to Barati et al. (2011), GNDVI measures chlorophyll content more accurately than NDVI. The formula for GNDVI is expressed as:

$$GNDVI = (NIR - Green) / (NIR + Green) \quad (7)$$

GNDVI values range from −1 to +1, with higher values indicating denser and healthier vegetation cover. Similar to NDVI, GNDVI is sensitive to changes in vegetation density, health, and photosynthetic activity, making it a valuable tool for monitoring vegetation dynamics and ecosystem health.

2.4.5. Ratio vegetation index (RVI)

The RVI is a vegetation index that measures the ratio of reflectance in two different spectral bands, typically the NIR and red bands. It is a simple yet effective index for assessing vegetation density and health. RVI values typically range from 0 to positive infinity. Higher RVI values indicate denser and healthier vegetation cover, while lower values suggest sparse or non-vegetated areas. The RVI is calculated as:

$$RVI = NIR / Red \quad (8)$$

2.4.6. Optimized soil adjusted vegetation index (OSAVI)

The OSAVI is a vegetation index similar to SAVI but optimized to provide better sensitivity to vegetation changes and reduced sensitivity to soil background variations. OSAVI is particularly useful in areas with diverse soil types or varying soil moisture conditions. The formular for OSAVI is expressed as:

$$OSAVI = 1.16 * (NIR - Red) / (NIR + Red + 0.16) \quad (9)$$

OSAVI utilizes a standard value of 0.16 for the canopy background adjustment factor, determined by Rondeaux et al. (1996) to be optimal for providing greater sensitivity to vegetation changes while reducing the influence of soil background variations. This adjustment allows OSAVI to effectively distinguish between low vegetation cover and areas with greater vegetation density, making it a valuable tool for vegetation monitoring and assessment.

2.4.7. Green chlorophyll index (GCI)

The GCI is a vegetation index that quantifies the chlorophyll content of vegetation based on the reflectance in the green spectral band. It is particularly useful for assessing plant health and physiological status, as chlorophyll is a key pigment involved in photosynthesis. GCI values typically range from negative to positive values. Higher positive GCI values indicate higher chlorophyll content and healthier vegetation, while negative values may indicate stress or senescence. The formula for GCI is expressed as:

$$GCI = ((NIR / Green)) - 1 \quad (10)$$

3. Results and Discussion

3.1. Vegetation indices distributions

The spatial distribution of different vegetation indices, as depicted in Fig. 2A–G, provides valuable insights into the variability of vegetation cover and associated environmental conditions across the study area. Fig. 2A depict the NDVI values, ranging from −0.05 to 0.44, indicating spatial variability in vegetation density and health. Areas with higher NDVI values correspond to regions with dense vegetation cover while areas with lower NDVI values represent urbanized regions with sparse vegetation or impervious surfaces.

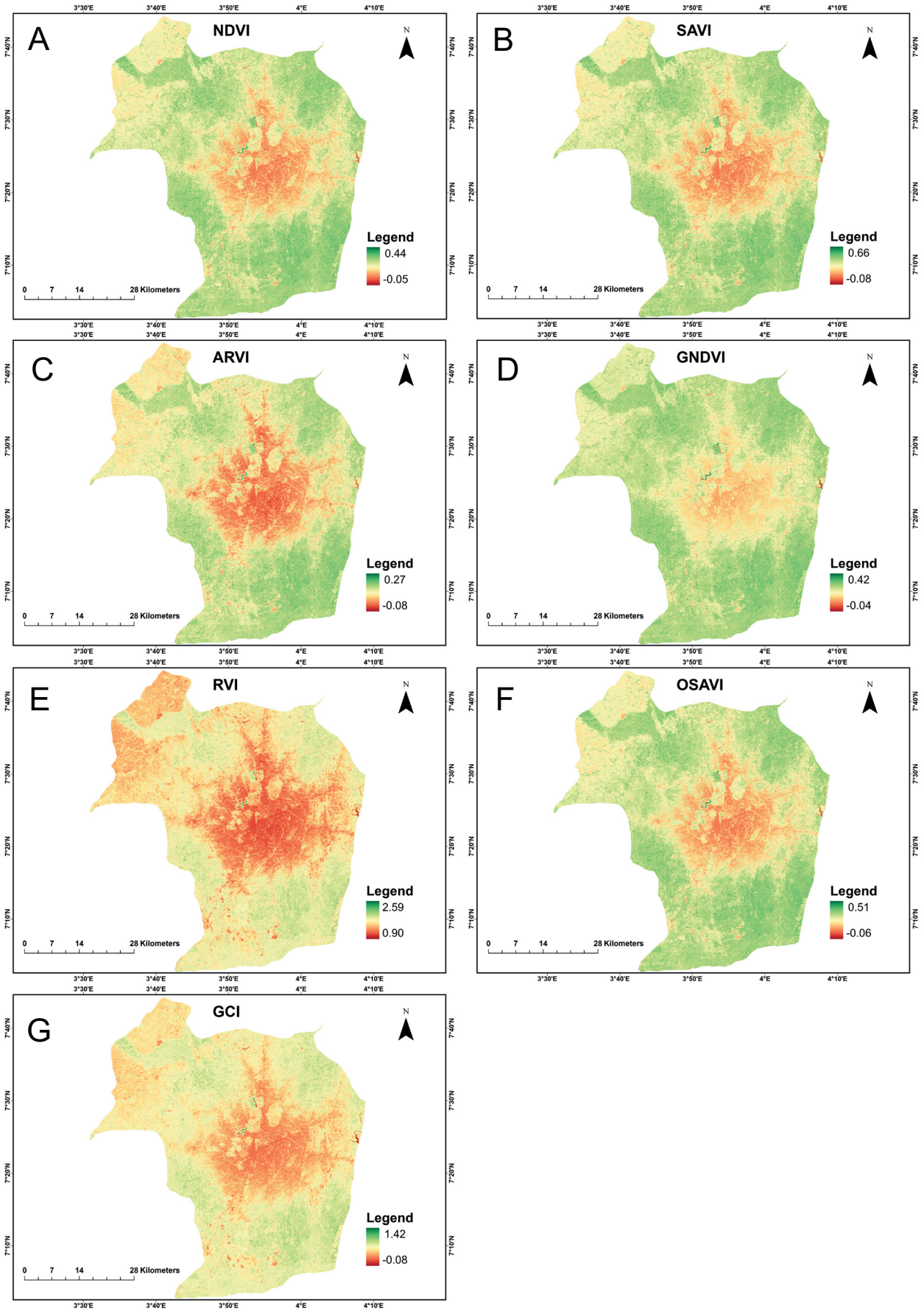

Figure 2. Spatial distribution of vegetation indices. **A** NDVI **B** SAVI **C** ARVI **D** GNDVI **E** RVI **F** OSAVI **G** GCI.

Fig. 2B illustrates the SAVI index with a range spanning from −0.08 to 0.66. This index clarifies variations in vegetation density and soil brightness, with positive values indicating vegetated areas exhibiting higher density, while negative values denote regions dominated by non-vegetated surfaces in the study area. The ARVI index (Fig. 2C) ranging from −0.08 to 0.27 offers insights into both vegetation density and atmospheric correction effects, with higher values indicative of healthier vegetation cover, while lower values hint at areas susceptible to atmospheric interference or exhibiting sparse vegetation. GNDVI values (Fig. 2D) range from −0.04 to 0.42, with higher values indicating greater vegetation density and health. Similar to NDVI, higher GNDVI values suggest areas with dense vegetation cover, while lower values indicate urban areas with limited vegetation. RVI values (Fig. 2E) range from 0.90 to 2.59, reflecting variations in vegetation vigor and canopy structure. Higher RVI values typically indicate denser and more vigorous vegetation, while lower values suggest sparse vegetation. Fig. 2F reveals the OSAVI index values ranging from −0.06 to 0.51, with positive values indicating the presence of vegetation. Higher OSAVI values indicate areas with denser vegetation cover, while negative values indicate areas with sparse vegetation. GCI index values (Fig. 2G) range from −0.08 to 1.42, reflecting variations in chlorophyll content and vegetation health. Higher GCI values typically indicate areas with healthier vegetation and higher chlorophyll content, while lower values indicates areas with less vigorous vegetation.

The spatial distribution of vegetation indices Fig. 2A–G also illustrates a notable trend of generally increasing values with greater distance from the core towards the periphery of the study area. This spatial pattern can be attributed to a combination of factors influencing land use, vegetation dynamics, and human activities across different regions.

In the core areas of the study area, including Ibadan North, Ibadan North-West, Ibadan South-West, Ibadan North-East, and Ibadan South-East, higher levels of land use intensity are prevalent due to extensive urban development, industrial activities, and transportation networks. These anthropogenic pressures have resulted in the removal of natural vegetation cover and the proliferation of impervious surfaces, negatively impacting vegetation health and density. As a consequence, these urbanized cores exhibit lower vegetation indices compared to peripheral regions. Conversely, peripheral areas such as parts of Ona Ara, Lagelu, and Oluyole comprise natural landscapes, rural settlements, and agricultural lands characterized by higher vegetation density and reduced human disturbance. These regions are endowed with more intact ecosystems and a greater diversity of vegetation cover. The presence of green spaces, agricultural activities, and less impervious surfaces contribute to healthier and more diverse vegetation communities, resulting in higher vegetation indices.

3.2. Land surface temperature

Fig. 3 illustrates the spatial distribution of LST across the study area, revealing a pronounced UHI effect within the area. The estimated LST values span from 28°C to 39°C, with a mean temperature of 34.8°C. The map distinctly identifies six prominent hotspots: Ibadan North, Ibadan North-West, Ibadan South-West, Ibadan North-East, Ibadan South-East, and outskirt of Ido. These areas experience elevated temperatures primarily due to sparse vegetation cover, inten-

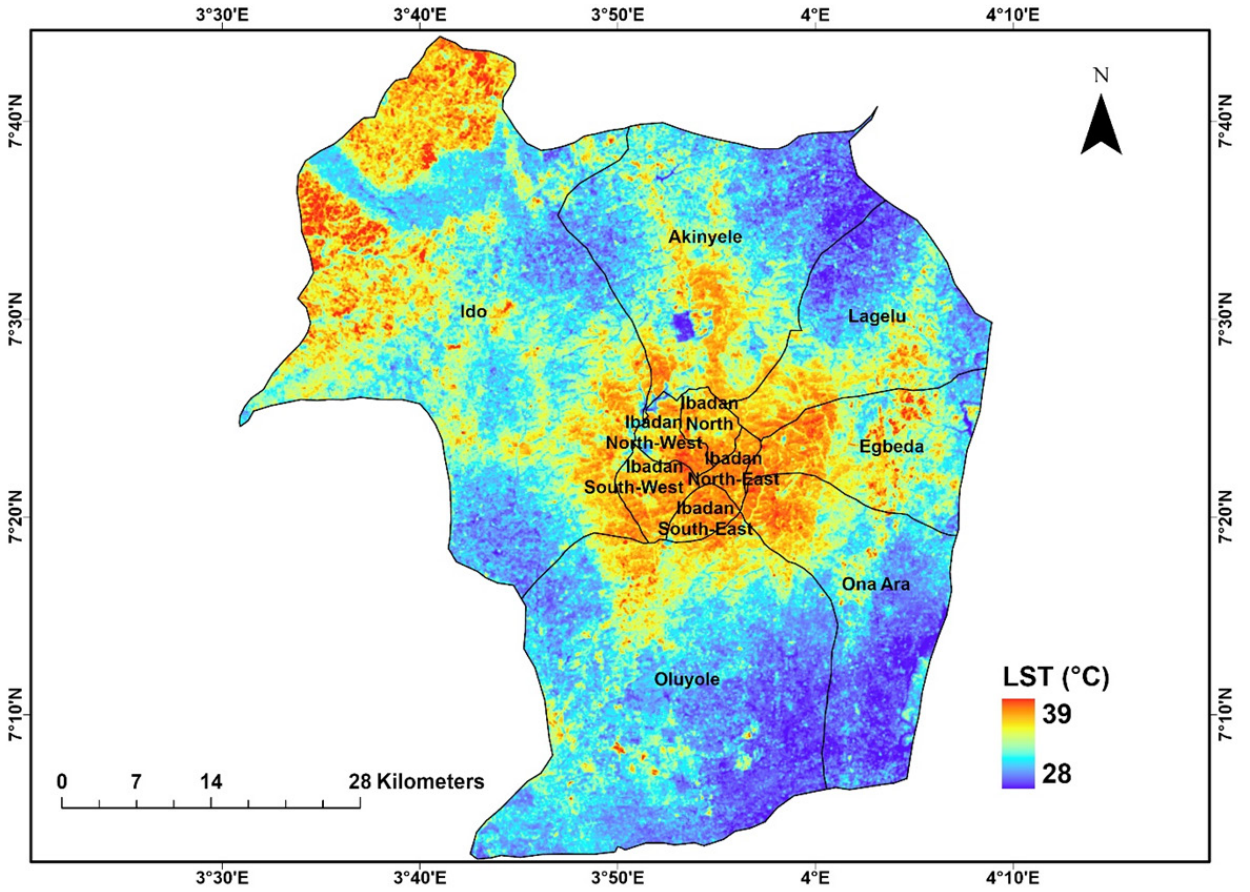

Figure 3. Land surface temperature.

Figure 4. Dense building structures at the core of the study area (Adeosun 2015).

sified by the release of urban anthropogenic heat and the insulating effect of dense building structures (Fig. 4).

3.3. Correlation analysis of LST and vegetation indices

To explore the correlation between vegetation indices and LST, a total of 1245 randomly selected sample points from LST, NDVI, SAVI, ARVI, GNDVI, RVI, OSAVI, and GCI images were utilized. Regression analysis was conducted, and the results were visually represented using 2D scatterplots (Fig. 5A–G). Table 3

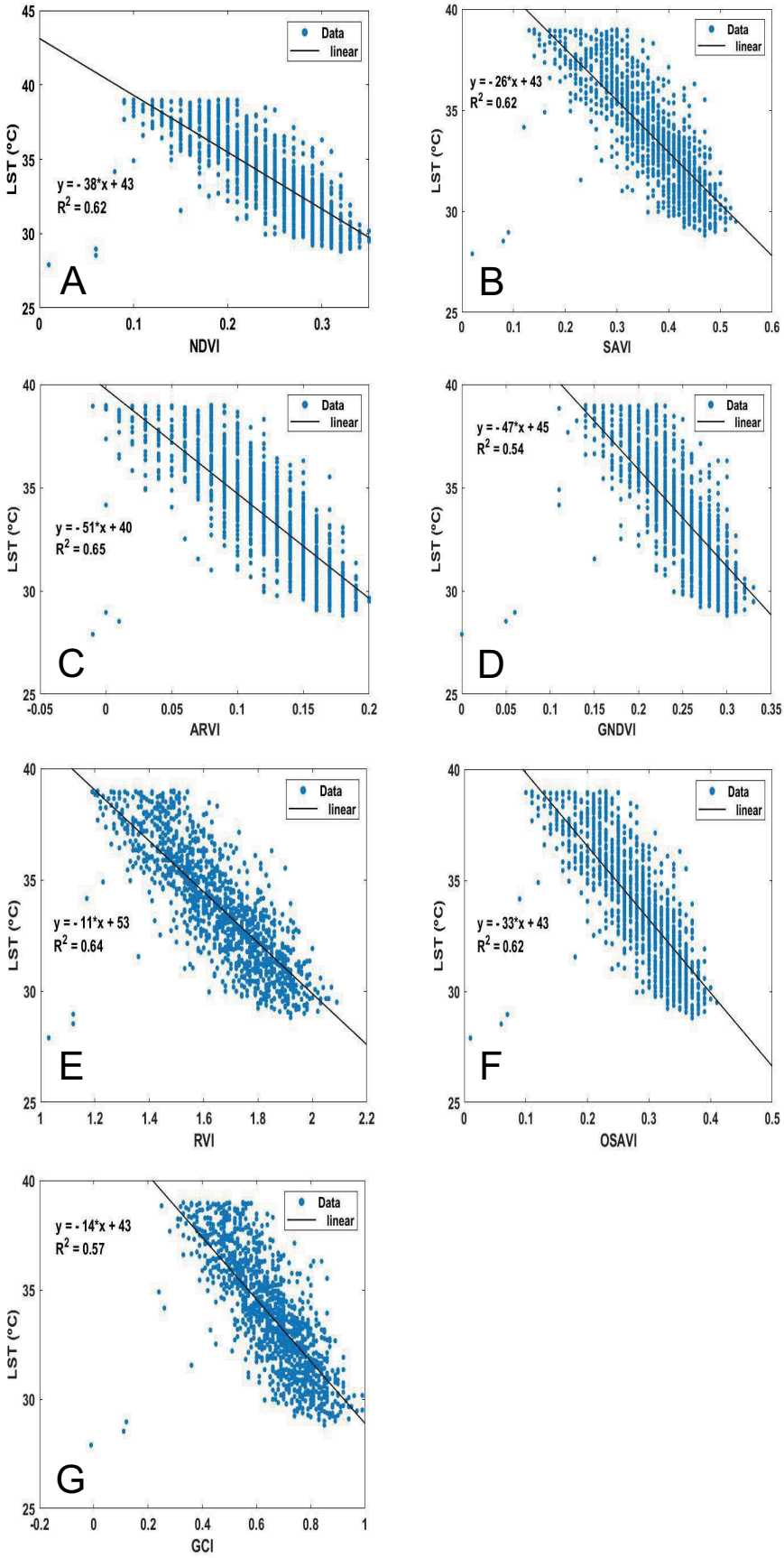

Figure 5. Vegetation indices and LST correlation. **A** NDVI/LST **B** SAVI/LST **C** ARVI/LST **D** GNDVI/LST **E** RVI/LST **F** OSAVI/LST **G** GCI/LST.

Table 3. Statistics of vegetation indices and LST relationship.

Statistics	NDVI/ LST	SAVI/ LST	ARVI/ LST	GNDVI/ LST	RVI/ LST	OSAVI/ LST	GCI/ LST
Standard deviation	1.588	1.588	1.529	1.754	1.542	1.594	1.698
R	−0.787	−0.787	−0.805	−0.732	−0.801	−0.786	−0.752
R^2	0.620	0.620	0.647	0.536	0.642	0.617	0.565
P	2.720E-263	2.986E-263	1.345E-283	1.447E-209	3.163E-279	2.139E-261	3.348E-227

presents the calculated standard deviation, Pearson correlation coefficients (*R*), coefficient of determination (R^2), and corresponding *P*-values.

Statistical analysis revealed a significant relationship between vegetation indices and LST at a significance level of $P < 0.01$. This indicates that the influence of vegetation indices on LST is statistically significant.

Among the indices examined, ARVI emerges as the most robust indicator of the relationship between vegetation indices and LST. ARVI exhibits the highest R^2 value among all indices analyzed, with an R^2 value of 0.647, a strong negative correlation as evidenced by its high absolute R-value of -0.8046, and the least standard deviation value of 1.529. This indicates that ARVI explains approximately 64.7% of the variability in LST within the study area. The high explanatory power of ARVI suggests that changes in ARVI values correspond closely to variations in LST, making it a reliable predictor of surface temperature dynamics. This can be attributed to the fact that ARVI incorporates atmospheric resistance into its formulation, making it less sensitive to atmospheric influences such as aerosols and water vapor. By accounting for atmospheric effects, ARVI provides a more accurate representation of vegetation properties and reduces the potential for confounding factors to distort the relationship between vegetation indices and LST. Prior study by Somvanshi and Kumari (2020) also highlighted the effectiveness of ARVI in capturing vegetation dynamics and surface temperature variations in urban environments. The established utility of ARVI in urban heat island studies and ecosystem monitoring further validates its suitability for analyzing the relationship between vegetation and LST in rapidly urbanizing areas.

According to the obtained results, the higher standard deviation, lower R-values and R^2 values observed for GNDVI and GCI suggest that these indices are less effective in explaining variations in LST compared to other vegetation indices in the study area. This can be attributed to the fact that GNDVI and GCI are more sensitive to environmental factors other than vegetation density, such as soil properties, atmospheric conditions, or urban infrastructure.

The results of our analysis reveal compelling insights into the dynamics between vegetation cover and surface temperature within the study area. Across a range of vegetation indices, including NDVI, SAVI, ARVI, GNDVI, RVI, OSAVI, and GCI, we observed consistent patterns indicative of the influence of vegetation on surface temperature dynamics. The negative R-values obtained for all vegetation indices underscore the inverse relationship between vegetation density and LST. These negative R-values, ranging from −0.732 to −0.805, indicate a moderate to strong negative linear relationship between vegetation indices and LST. This suggests that as vegetation density increases, land surface

temperature tends to decrease likewise as vegetation density decrease, land surface temperature tends to increase. This finding aligns with the expected behaviour in urban environments, where areas with denser vegetation typically experience lower surface temperatures due to the cooling effects of vegetation, such as shading and evapotranspiration.

Furthermore, the R^2 values obtained for each vegetation index provide valuable insights into the explanatory power of vegetation dynamics in predicting variations in LST. With R^2 values ranging from 0.536 to 0.647, our analysis indicates that between 53.6% and 64.7% of the variability in LST can be attributed to changes in vegetation cover as captured by the corresponding vegetation index. This highlights the significant contribution of vegetation dynamics to surface temperature variations within the study area

These findings have important implications for urban planning and climate resilience efforts. By recognizing the pivotal role of vegetation in mitigating UHI, policymakers and urban planners can prioritize strategies aimed at preserving and enhancing urban green spaces. Implementing measures such as increasing tree canopy cover, and promoting green infrastructure initiatives can help mitigate the adverse effects of urbanization on local climate and improve the quality of life for urban residents.

4. Conclusion

The study provides valuable insights into the complex relationship between remote sensing-based vegetation indices and LST in a rapidly urbanizing environment. Through quantitative analysis of satellite imagery and regression modeling, we have explored the dynamics of vegetation cover and its impact on UHI in the Ibadan region. Utilizing seven vegetation indices to assess their correlations with LST, we uncovered essential patterns shaping LST distribution across both urban and peri-urban landscapes. The results of this study underscore the pivotal role of vegetation density in shaping LST distributions. Notably, we observed a robust negative correlation between vegetation indices and LST, with the ARVI index exhibiting the strongest association among the indices examined. This suggests that variations in vegetation density significantly moderate surface temperatures. Urban cores within the study area exhibit lower vegetation density and higher LST values, attributable to intense land use, anthropogenic heat release, and limited green spaces. In contrast, peripheral regions within the study area demonstrate higher vegetation indices and lower LST values, reflecting healthier vegetation cover and reduced UHI effects.

Our study challenges the conventional reliance on the NDVI as the sole indicator of vegetation abundance in remote sensing studies investigating the vegetation-LST relationship. We highlight the necessity for a more comprehensive approach, incorporating multiple vegetation indices to better capture the variations of vegetation dynamics and their impact on LST. Furthermore, this study highlights the importance of remote sensing techniques in monitoring urban environmental dynamics and informing sustainable urban planning strategies. By leveraging multispectral satellite imagery and quantitative analysis, policymakers can identify areas vulnerable to heat stress and prioritize interventions to enhance urban green infrastructure, resilience to climate change, and mitigate UHI effects.

References

Adeosun O (2015) Urbanization in Ibadan [Photograph]. Flickr. https://www.flickr.com/photos/adeosun_olamide/22728963295

Aliyu AO, Youngu TT, Bala A, Azua S, Bawa S, Agboola MK (2022) Relationship of the seasonal vegetation indices against the NDVI and LST in the region of Kamuku Game Reserve and Kwiambana National Park, Nigeria. Indonesian Journal of Earth Sciences 2(2): 203–225. https://doi.org/10.52562/injoes.v2i2.409

Barati S, Rayegani B, Saati M, Sharifi A, Nasri M (2011) Comparison of the accuracies of different spectral indices for estimation of vegetation cover fraction in sparse vegetated areas. The Egyptian Journal of Remote Sensing and Space Sciences 14(1): 49–56. https://doi.org/10.1016/j.ejrs.2011.06.001

Bhagyanagar R, Kawal BM, Dwarakish GS, Surathkal S (2012) Land use/land cover change and urban expansion during 1983–2008 in the coastal area of Dakshina Kannada district, South India. Journal of Applied Remote Sensing 6(1): 063576-1. https://doi.org/10.1117/1.JRS.6.063576

Brattebo BO, Booth DB (2003) Long-term stormwater quantity and quality performance of permeable pavement systems. Water Research 37(18): 4369–4376. https://doi.org/10.1016/S0043-1354(03)00410-X

Castaldi F (2021) Sentinel-2 and Landsat-8 Multi-Temporal Series to Estimate Topsoil Properties on Croplands. Remote Sensing 13(17): 3345. https://doi.org/10.3390/rs13173345

Das N, Mondal P, Sutradhar S, Ghosh R (2020) Assessment of variation of land use/land cover and its impact on land surface temperature of Asansol subdivision. The Egyptian Journal of Remote Sensing and Space Science 24(1): 131–149. https://doi.org/10.1016/j.ejrs.2020.05.001

Debele GB, Beketie KT (2024) Studying the spatial non-stationary relationships of some physical parameters on the Earth's surface temperature using GWR in Upper Awash basin, Ethiopia. Scientific African 23: e02052. https://doi.org/10.1016/j.sciaf.2023.e02052

Dontree S (2010) Relation of land surface temperature (LST) and land use/land cover (LULC) from remotely sensed data in Chiang Mai-Lamphun basin. In: SEAGA Online Proceedings. The 2010 Southeast Asian Geography Conference (SEAGA), Hanoi (Vietnam), November 2010.

Fashae OA, Adagbasa EG, Olusola AO, Obateru RO (2020) Land use/land cover change and land surface temperature of Ibadan and environs, Nigeria. Environmental Monitoring and Assessment 192(2): 109. https://doi.org/10.1007/s10661-019-8054-3

Firozjaei MK, Alavipanah SK, Liu H, Sedighi A, Mijani N, Kiavarz M, Weng Q (2019) A PCA–OLS Model for Assessing the Impact of Surface Biophysical Parameters on Land Surface Temperature Variations. Remote Sensing 11(18): 2094. https://doi.org/10.3390/rs11182094

Gitelson AA, Viña A, Arkebauer TJ, Rundquist DC, Keydan G, Leavitt B (2003) Remote estimation of leaf area index and green leaf biomass in maize canopies. Geophysical Research Letters 30(5). https://doi.org/10.1029/2002GL016450

Gogoi PP, Vinoj V, Swain D, Roberts G, Dash J, Tripathy S (2019) Land use and land cover change effect on surface temperature over Eastern India. Scientific Reports 9(1): 1–10. https://doi.org/10.1038/s41598-019-45213-z

Grimmond S (2007) Urbanization and global environmental change: local effects of urban warming. Geographical Journal 173(1): 83–88. http://www.jstor.org/stable/30113496

Guechi I, Gherraz H, Alkama D (2021) Correlation analysis between biophysical indices and Land Surface Temperature using remote sensing and GIS in Guelma city (Algeria). Bulletin de la Societe Royale des Sciences de Liege 90: 158–180. https://doi.org/10.25518/0037-9565.10457

Gutman G, Skakun S, Gitelson A (2021) Revisiting the use of red and near-infrared reflectances in vegetation studies and numerical climate models. Science of Remote Sensing 4: 100025. https://doi.org/10.1016/j.srs.2021.100025

Huete AR (1988) A soil-adjusted vegetation index (SAVI). Remote Sensing of Environment 25(3): 295–309. https://doi.org/10.1016/0034-4257(88)90106-X

Kumar D, Shekhar S (2015) Statistical analysis of land surface temperature–vegetation indexes relationship through thermal remote sensing. Ecotoxicology and Environmental Safety 121: 39–44. https://doi.org/10.1016/j.ecoenv.2015.07.004

Kumar KS, Bhaskar PU, Padmakumari K (2012) Estimation of land surface temperature to study urban heat island effect using LANDSAT ETM+ image. International Journal of Engineering, Science and Technology 4(2): 771-778.

Liu L, Zhang Y (2011) Urban heat island analysis using the Landsat TM data and ASTER data: A case study in Hong Kong. Remote Sensing 3(7): 1535–1552. https://doi.org/10.3390/rs3071535

Macarof P, Groza S, Statescu F (2018) Investigating correlation lst and vegetation indices using landsat images for the warmest month: a case study of Lasi County. Annals of Valahia University of Targoviste. Geographical Series 18(1): 33–40.

MacLachlan A, Biggs E, Roberts G, Boruff B (2017) Urbanisation-induced land cover temperature dynamics for sustainable future urban heat island mitigation. Urban Science 1(4): 38. https://doi.org/10.3390/urbansci1040038

Pearson RL, Miller LD (1972) Remote mapping of standing crop biomass for estimation of the productivity of the shortgrass prairie, Pawnee National Grasslands, Colorado. Proceedings of the 8th International Symposium on Remote Sensing of the Environment 2: 1355–1379.

Plocoste T, Jacoby-Koaly S, Molinié J, Petit R (2014) Evidence of the effect of an urban heat island on air quality near a landfill. Urban Climate 10: 745–757. https://doi.org/10.1016/j.uclim.2014.03.007

Population Stat (2024) Estimated population of Ibadan. In World statistical data. https://populationstat.com/nigeria/ibadan

Rondeaux G, Steven M, Baret F (1996) Optimization of soil-adjusted vegetation indices. Remote Sensing of Environment 55(2): 95–107. https://doi.org/10.1016/0034-4257(95)00186-7

Rouse JW, Haas RH, Schell JA, Deering DW, Harlan JC (1974) Monitoring the Vernal Advancement or Retrogradation of Natural Vegetation. NASA/GSFC, Type III, Final report, Greenbelt, MD, 371 pp.

Schwarz N, Schlink U, Franck U, Großmann K (2012) Relationship of land surface and air temperatures and its implications for quantifying urban heat island indicators—an application for the city of Leipzig (Germany). Ecological Indicators 18: 693–704. https://doi.org/10.1016/j.ecolind.2012.01.001

Sobrino JA, Jiménez-Muñoz JC, Paolini L (2004) Land surface temperature retrieval from LANDSAT TM 5. Remote Sensing of Environment 90(4): 434–440. https://doi.org/10.1016/j.rse.2004.02.003

Somvanshi SS, Kumari M (2020) Comparative analysis of different vegetation indices with respect to atmospheric particulate pollution using sentinel data. Applied Computing and Geosciences 7: 100032. https://doi.org/10.1016/j.acags.2020.100032

Tan J, Yu D, Li Q, Tan X, Zhou W (2020) Spatial relationship between land use/land-cover change and land surface temperature in the Dongting Lake area, China. Scientific Reports 10(1): 1–9. https://doi.org/10.1038/s41598-020-66168-6

Tanré D, Holben BN, Kaufman YJ (1992) Atmospheric correction algorithm for NOAA-AVHRR products: Theory and application. IEEE Transactions on Geoscience and Remote Sensing 30(2): 231–248. https://doi.org/10.1109/36.134074

Ullah W, Ahmad K, Ullah S, Tahir AA, Javed MF, Nazir A, Abbasi AM, Aziz M, Mohamed A (2023) Analysis of the relationship among land surface temperature (LST), land use land cover (LULC), and normalized difference vegetation index (NDVI) with topographic elements in the lower Himalayan region. Heliyon 9(2): e13322. https://doi.org/10.1016/j.heliyon.2023.e13322

United Nations, Department of Economic and Social Affairs, Population Division (2018). World Urbanization Prospects: The 2018 Revision (ST/ESA/SER.A/420). New York, United Nations.

United States Geological Survey (USGS) (2024) Landsat Missions: Landsat Science Products https://www.usgs.gov/land-resources/nli/landsat/landsat-science-products [Accessed on 15.02.2024]

Wang X (2023) Remote Sensing Applications to Climate Change. Remote Sensing 15(3): 747. https://doi.org/10.3390/rs15030747

Wang YC, Hu BK, Myint SW, Feng CC, Chow WT, Passy PF (2018) Patterns of land change and their potential impacts on land surface temperature change in Yangon, Myanmar. Science of the Total Environment 643: 738–750. https://doi.org/10.1016/j.scitotenv.2018.06.209

Wei MA, Yun-hao C, Ji Z (2008) Quantitative analysis of land surface temperature-vegetation indexes relationship based on remote sensing. The International Archives of the Photogrammetry, Remote Sensing and Spatial Information Sciences 37(B6b): 261–264.

Yue W, Xu J, Tan W, Xu L (2007) The relationship between land surface temperature and NDVI with remote sensing: application to Shanghai Landsat 7 ETM+ data. International Journal of Remote Sensing 28(15): 3205–3226. https://doi.org/10.1080/01431160500306906

Zaeemdar S, Baycan T (2017) Analysis of the Relationship between Urban Heat Island and Land Cover in Istanbul through Landsat 8 OLI. Journal of Earth Science & Climatic Change 8(11): 423. https://doi.org/10.4172/2157-7617.1000423

Additional information

Conflict of interest

No conflict of interest was declared.

Ethical statement

No ethical statement was reported.

Funding

No funding was reported.

Author contributions

All authors have contributed equally.

Author ORCIDs

Ibrahim Olatunji Raufu https://orcid.org/0000-0003-3474-8618

Data availability

All of the data that support the findings of this study are available in the main text or Supplementary Information.